Simple relation between lidar multiple scattering and depolarization for water clouds

Yongxiang Hu, Zhaoyan Liu, David Winker, Mark Vaughan, and Vincent Noel
Climate Science Branch, NASA Langley Research Center, Hampton, Virginia 23681

Luc Bissonnette and Gilles Roy
DRDC Valcartier, 2459 Pie-XI Blvd. North, Val-Belair, Quebec, Canada G3J 1X5

Matthew McGill
Code 613.1, NASA's Goddard Space Flight Center, Greenbelt, Maryland 20771

Received February 2, 2006; revised March 26, 2006; accepted March 27, 2006; posted April 3, 2006 (Doc. ID 67755)

An empirical relationship is derived between the multiple-scattering fraction and the linear depolarization ratio by using Monte Carlo simulations of water clouds measured by backscatter lidar. This relationship is shown to hold for clouds having a wide range of extinction coefficients, mean droplet sizes, and droplet size distribution widths. The relationship is also shown to persist for various instrument fields of view and for measurements made within broken cloud fields. The results obtained from the Monte Carlo simulations are verified by using multiple-field-of-view lidar measurements. For space-based lidars equipped to measure linear depolarization ratios, this new relationship can be used to accurately assess signal perturbations due to multiple scattering within nonprecipitating water clouds. © 2006 Optical Society of America
OCIS code: 010.0010.

Water clouds may serve as targets for testing lidar measurements. Because of the very small mean free path for photon scattering typical of water clouds, lidar backscatter measurements always contain contributions from multiple scattering, which affect lidar data analysis. In this Letter we introduce a polynomial approximation, derived via Monte Carlo simulations, that provides a highly accurate description of the relationship between the linear depolarization of the 180°-backscatter signal and the fraction of multiple scattering present in the signal. The validity of the relationship is demonstrated by using multiple-field-of-view (MFOV) lidar backscatter measurements made by using the Defense R&D Canada Valcartier lidar.[1]

Single scattering from spherical droplets in the 180°-backscatter direction retains the polarization of the incident light, but scattering at other scattering angle alters the polarization state. Thus, for a lidar transmitting a linearly polarized beam, the single-backscatter signal from a water cloud is also linearly polarized, and depolarization of the signal can be attributed to multiple-scattering effects.[2] To investigate the relation between multiple scattering and depolarization ratios, we define two scattering parameters. We term the first one the accumulated single-scattering fraction, $A_S(r)$, such that

$$A_S(r) = I_S(r)/I_T(r), \tag{1}$$

where $I_T(r) = \int_{r_0}^{r} X_T(r')\mathrm{d}r'$ and $I_S(r) = \int_{r_0}^{r} X_S(r')\mathrm{d}r'$ are, respectively, the integrated, range-corrected single-scattering (X_S) and total-scattering (X_T = single + multiple) lidar backscatter signals computed over the range r_0 to r, where r_0 is the near-range boundary of the cloud being measured (i.e., r_0 is the cloud base for up-looking systems and the cloud top for down-looking lidars). Similarly, we also define the accumulated depolarization ratio, $\delta_{\mathrm{acc}}(r)$, such that

$$\delta_{\mathrm{acc}}(r) = I_{T,\perp}(r)/I_{T,\parallel}(r), \tag{2}$$

where $I_{T,\parallel}(r)$ and $I_{T,\perp}(r)$ represent, respectively, the components of the total-backscattered signal, X_T, polarized parallel and perpendicular to the polarization plane of the laser transmitter; that is, $I_{T,\parallel}(r) = \int_{r_0}^{r} X_{T,\parallel}(r')\mathrm{d}r'$ and $I_{T,\perp}(r) = \int_{r_0}^{r} X_{T,\perp}(r')\mathrm{d}r'$. The relationship between δ_{acc} and A_s, never systematically assessed in the past owing to the lack of accurate depolarization simulations, was investigated via a Monte Carlo study that examined simulated lidar backscatter signals derived from a number of different water cloud models.

A standard Mie scattering code[3] was used to compute the single-scattering matrices for nonprecipitating (spherical) water cloud droplets. These in turn provided the necessary inputs for the full Stokes vector Monte Carlo code[4] that was used to generate the simulated multiple-scattering signals. To ensure a thorough examination of the underlying physics, hundreds of measurement scenarios were modeled. These scenarios include a diverse set of cloud physical and optical properties, combined with a number of different lidar fields-of-view (FOVs). The water clouds were parametrized by using extinction coefficients ($\sigma = 1$ km^{-1} to $\sigma = 100$ km^{-1}) and effective radii ($R_e = 4$ μm to $R_e = 12$ μm), and the widths of the (assumed) Gamma distribution for droplet sizes ($\gamma = 3$ to $\gamma = 25$). The gamma distribution is used throughout this study, as it has been shown to provide a realistic representation of the actual droplet size distributions in water clouds.[5] Broken clouds are also considered. Because the amount of multiple scattering present in the lidar backscatter signal strongly depends on the

0146-9592/06/121809-3/$15.00

receiver's FOV, this parameter was also varied (FOV of 0.04–1.3 mrad for space-based lidar) within the simulation. The geometric thickness of the modeled clouds was 0.2–1 km. The space-based lidar is assumed to have a range to the cloud of 700 km. Simulations were also performed on ground-based measurements (cloud-based height 0.7 km) with FOV up to 16 mrad.

A plot of representative $A_S(r)$ and $\delta_{acc}(r)$ values derived from the simulations is shown in Fig. 1. The individual symbols represent the results obtained for 14 separate cases from among the complete set of simulation results. In each of these cases, the simulation from which the $A_S(r)$ and $\delta_{acc}(r)$ values were computed used a different combination of extinction coefficient (σ), mean particle size (R_e), Gamma size distribution widths (γ), and lidar FOV. Also included among the example cases are two instances of broken clouds (see cases 8 and 9, for which the cloud fraction is less than 1.0) and five cases of ground-based lidar (see cases 9–14). The exact parametrizations used for each case are listed in Table 1.

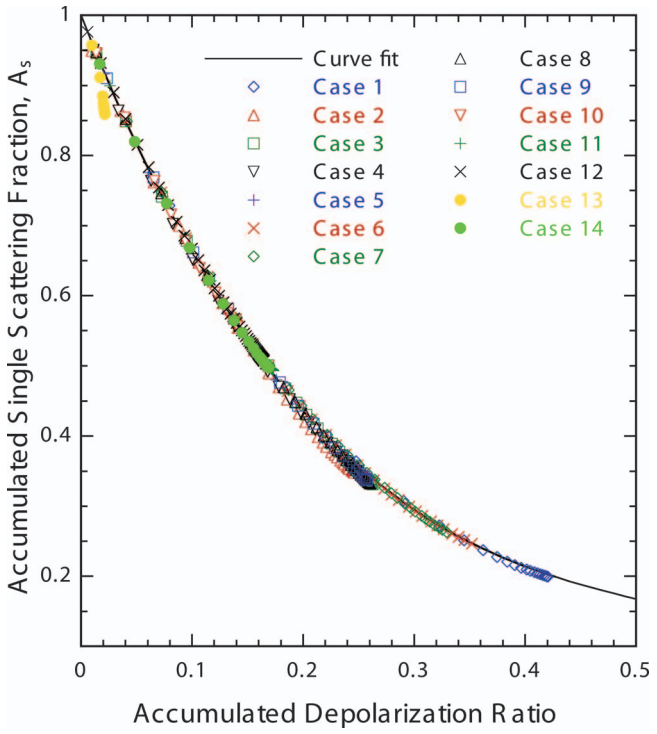

Fig. 1. Empirically derived relation between A_s and δ_{acc}. The relation is valid for a variety of extinction coefficients, particle size distributions, cloud geometries, and lidar FOVs.

Examining the 14 cases shown in Fig. 1 (each is plotted with a unique symbol, and multiple points for each case are for different ranges into the cloud layer), it is obvious that there is a simple relation between the accumulated single-scattering fraction, $A_S(r)$, and the accumulated depolarization ratio, $\delta_{acc}(r)$. The solid curve represents a third-order polynomial least-squares fit to the entire set of $A_S(r)$ and $\delta_{acc}(r)$ data pairs derived from all of the simulations. The good agreement between these examples and the least-squares fit is shared by all the space-based lidar cases simulated, regardless of cloud microphysics, macrophysics, and lidar FOV. For $\delta_{acc} < 0.5$, the exact functional relationship between the two scattering parameters is given by

$$A_s = 0.999 - 3.906\delta_{acc} + 6.263\delta_{acc}^2 - 3.554\delta_{acc}^3. \quad (3)$$

By applying Eq. (3) to the lidar backscatter profiles generated in this simulation study, the multiple-scattering contributions to the signals can be estimated and removed with the smoothly varying water cloud depolarization data. When the single-scattering approximations derived by using Eq. (3) are compared with the known-truth record for each simulation, the corrected profiles are found to be within 2% of the true values for all space-based lidar cases and for most ground-based lidar cases with relatively large FOVs. Equation (3) is less accurate for ground-based lidar cases with footprint sizes less than 3 m.

Validation of Eq. (3) was accomplished by using field measurements of water clouds acquired by the MFOV lidar on December 6, 1999. Examples of water

Table 1. Model Parameters for Simulation Results Shown in Fig. 1

Case	Wavelength (nm)	Ground/ Space	R_e (μm)	γ	τ	FOV (mrad)	Cloud Fraction
1	532	Space	4	6	20	0.13	1.0
2	532	Space	8	16	8	0.13	1.0
3	532	Space	8	6	8	0.13	1.0
4	1064	Space	8	6	8	0.13	1.0
5	1064	Space	4	25	8	0.13	1.0
6	532	Space	4	6	8	1.3	1.0
7	532	Space	4	6	8	0.04	1.0
8	532	Space	4	6	8	0.13	0.5
9	532	Space	4	6	8	0.13	0.3
10	1064	Ground	4	6	8	12	1.0
11	532	Ground	8	6	16	12	1.0
12	532	Ground	3	6	10	16	1.0
13	532	Ground	8	6	16	0.5	1.0
14	1064	Ground	4	6	8	6	1.0

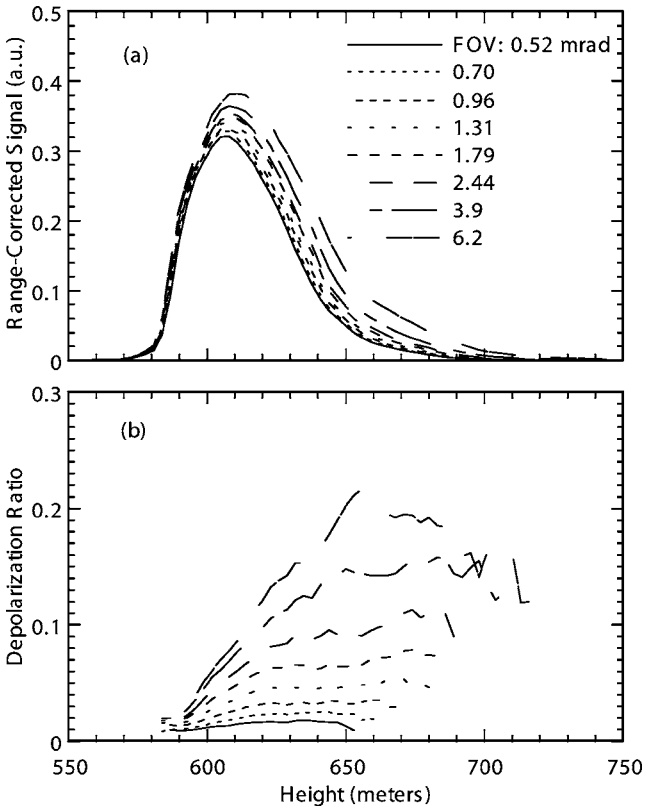

Fig. 2. Lidar profiles of eight different FOVs. (a) Range-corrected lidar backscatter profiles. (b) Corresponding depolarization ratio profiles.

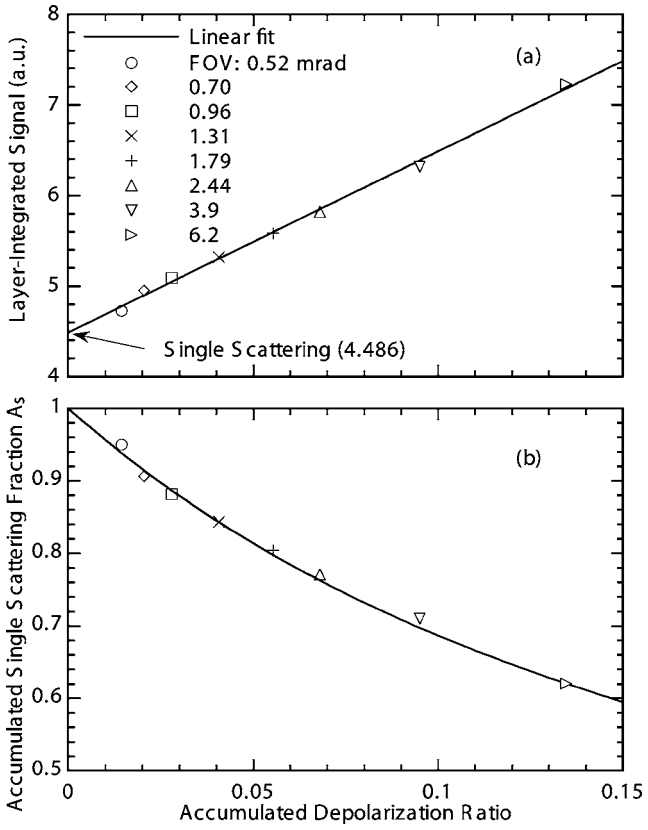

Fig. 3. (a) Deriving the single-scattering component from the MFOV lidar observations through extrapolations. (b) Comparison between the eight FOV lidar observations with the $A_s-\delta_{acc}$ relation of Eq. (3).

cloud measurements made by the lidar are provided in Fig. 2. Figure 2(a) presents the range-corrected signal profiles for all eight FOVs. Figure 2(b) shows the corresponding depolarization ratio profiles.

A plot of the layer integrated backscatter as a function of the layer integrated depolarization ratio, δ_{acc} (which can be derived directly), is shown in Fig. 3(a) for all eight FOV channels. As the relationship can be approximated by using a linear fit, we estimate the layer integrated single-scattering signal, $I_S(r)$, by extrapolating the MFOV integrated lidar backscatter signals to $\delta_{acc}=0$. The value obtained by this method (4.486, arbitrary units) is then used to derive the single-scattering fractions (A_s) for all FOVs. The resulting single-scattering fraction values, computed by integrating over the entire cloud layer, are shown in Figure 3(b), again as a function of the corresponding integrated depolarization ratio. The values computed from the lidar measurements are shown using symbols. Also shown (solid curve) are the approximations to A_S computed by using Eq. (3). Examination of the figure shows that the predicted values derived by using the polynomial approximation agree quite well with the lidar field observations.

The single-scattering profile derived by using this multiple-scattering correction technique has a number of potential applications. Most important, this approach can be used for calibration or validation of space-based lidar systems by comparing the integrated attenuated signals of optically thick water clouds (e.g., cloud optical depth greater than ~3) with the theoretical limit of $1/2S_c$, where S_c is the extinction-to-backscatter ratio.[6] For water clouds, S_c is known to have a stable value at the visible and near-infrared wavelengths.[7,8] Alternately, if the lidar is already well calibrated, the total column optical depth of thin clouds or aerosols above the water cloud layer can be accurately estimated.

This work is supported by the NASA radiation science program under Hal Maring and Don Anderson. Y. Hu's e-mail address is yongxiang.hu-1@nasa.gov.

References

1. L. R. Bissonnette, G. Roy, and F. Fabry, J. Atmos. Ocean. Technol. **18**, 1429 (2001).
2. K. Sassen and R. L. Petrilla, Appl. Opt. **25**, 1450 (1986).
3. W. Wiscombe, Appl. Opt. **19**, 1505 (1980).
4. Y. Hu, D. Winker, P. Yang, B. Baum, L. Poole, and L. Vann, J. Quant. Spectrosc. Radiat. Transf. **70**, 569 (2001).
5. N. J. Miles, J. Verlinde, and E. E. Clothiaux, J. Atmos. Sci. **57**, 295 (2000).
6. C. Platt, D. Winker, M. Vaughan, and S. Miller, J. Appl. Meteorol. **38**, 1330 (1999).
7. R. G. Pinnick, S. G. Jennings, P. Chylek, C. Ham, and W. T. Grandy, Jr., J. Geophys. Res. **88**, 6787 (1983).
8. E. J. O'Connor, A. Illingworth, and R. Hogan, J. Atmos. Ocean. Technol. **21**, 777 (2004).